Journal of Fluorescence, Vol. 16, No. 1, January 2006 (© 2006)
DOI: 10.1007/s10895-005-0019-y

Confocal Fluorescence Recovery After Photobleaching of Green Fluorescent Protein in Solution

Thomas J. Pucadyil[1] and Amitabha Chattopadhyay[1,2]

Received August 9, 2005; accepted September 27, 2005
Published online: January 6, 2006

Fluorescence recovery after photobleaching (FRAP) is one of the most widely used approaches to quantitatively estimate diffusion characteristics of molecules in solution and cellular systems. In general, comparison of the diffusion times ($t_{1/2}$) from a FRAP experiment provides qualitative estimates of diffusion rates. However, obtaining consistent and reliable quantitative estimates of mobility of molecules using FRAP is hindered by the lack of appropriate standards for calibrating the FRAP set-up (microscope configuration and data fitting algorithms) used in a given experiment. In comparison with other fluorescent markers, the green fluorescent proteins (GFP) possess characteristics that are ideal for use in such experiments. We have monitored the mobility of pure enhanced green fluorescent protein (EGFP) in a viscous solution by confocal FRAP experiments. Our experimentally determined diffusion coefficient of EGFP in a glycerol–water mixture is in excellent agreement with the value predicted for GFP in a solution of comparable viscosity, calculated using the Stokes–Einstein equation. The agreement in the experimentally determined diffusion coefficient and that predicted from theoretical framework improves significantly when one takes into account the effective size of the bleached spot in such experiments. Our results therefore validate the use of GFP as a convenient standard for FRAP experiments. Importantly, we present a simple method to correct for artifacts in the accurate determination of diffusion coefficient of molecules measured using FRAP arising due to the underestimation in the effective size of the bleached spot.

KEY WORDS: GFP; Confocal FRAP; lateral diffusion; bleached spot radii; glycerol–water mixture.

INTRODUCTION

Fluorescence recovery after photobleaching (FRAP) is a widely used technique in the quantitative analysis of diffusion characteristics of molecules in solution and cellular environments [1–6]. This approach involves generating a concentration gradient of fluorescent molecules by irreversibly photobleaching a fraction of fluorophores in the region of observation. The dissipation of this gradient with time due to diffusion of fluorophores into the bleached region from unbleached regions is an indicator of the mobility of fluorophores. A major requirement in such studies is the labeling of the molecule under investigation with an appropriate fluorophore [3]. Consequently, the application of FRAP along with the development of molecular biological techniques of engineering intrinsically fluorescent proteins covalently attached to molecules of interest [7] has resulted in a better understanding of molecular dynamics in cells and other complex assemblies [5].

Qualitative estimates of molecular mobility in a particular system can be obtained by comparing the characteristic diffusion times ($t_{1/2}$) of the recovery kinetics from a FRAP experiment that is usually adequate to characterize a specific dynamic phenomenon. However, a limitation in arriving at a consistent and reliable quantitative estimate of molecular mobility using FRAP is the lack

[1] Centre for Cellular and Molecular Biology, Uppal Road, Hyderabad, 500007, India.
[2] To whom correspondence should be addressed. E-mail: amit@ccmb.res.in

of appropriate standards to calibrate the FRAP set-up, which includes the microscope configuration and algorithms used for data analysis [4]. A review of the literature on application of FRAP shows that aqueous and/or water–glycerol mixtures of fluorophores such as fluorescein isothiocyanate (FITC) [8] and rhodamine-6G [9], or proteins with known molecular dimensions extrinsically labeled with fluorophores [8,10] have previously been used as possible standards for FRAP. The intrinsic limitation with such standards is the rather high mobility of molecules (10–100 $\mu m^2\ s^{-1}$) in aqueous solutions or in water–glycerol mixtures which would require high-power lasers to induce a significant extent of bleaching and/or to bleach a larger area in a short duration of time to enable the detection of the fast fluorescence recovery kinetics. In addition, commonly used fluorophores such as FITC are prone to quenching in solution in presence of molecular oxygen and display pH-dependent fluorescence characteristics, while probes such as rhodamine-6G readily adsorb to glass. Further, the use of fluorescently-derivatized proteins requires an additional purification step to separate unbound fluorophores from solution before they can be used in such experiments.

Green fluorescent protein (GFP) from the jellyfish *Aequoria victoria* and its variants have become popular reporter molecules for monitoring protein expression, localization, and mobility of various membrane and cytoplasmic proteins [7]. Importantly, tagging cellular proteins with GFP has allowed direct visualization of signaling and real-time trafficking in living cells [11,12]. GFP possesses characteristics that are highly desirable for use as reporter molecules [7,13]. These include its intrinsic, cofactor-independent fluorescence, which displays remarkable stability in the presence of denaturants and over a wide range of pH conditions. More importantly, mutants of GFP such as the S65T mutant [14] display enhanced brightness over the wild-type GFP [15] and are well characterized in terms of their photobleaching behavior [15,16]. The availability of the high-resolution structure of GFP [17] has enabled the prediction of the diffusion coefficient of GFP in a given medium using the Stokes–Einstein equation. The theoretically calculated diffusion coefficient of GFP in a viscous solution (equivalent to a 90% glycerol–water mixture) is 0.7 $\mu m^2\ s^{-1}$ [18]. Interestingly, this represents a value that is within the estimated range of diffusion of molecules in several model and biological membranes [19], and can be conveniently measured using currently available confocal microscopes with standard configurations for data acquisition. In the present report, we tested whether a viscous solution of the GFP variant, enhanced GFP (EGFP) [20], could represent a standard for FRAP measurements by comparing the experimentally measured diffusion coefficient to that predicted from the Stokes–Einstein equation, using a standard FRAP set-up.

EXPERIMENTAL

Materials

Purified EGFP (F64L, S65T [20]) was a generous gift from Prof. G. Krishnamoorthy (Tata Institute for Fundamental Research, Mumbai, India). Glycerol (molecular biology grade, >99% pure) was obtained from Biogene (San O Ramon, CA). All other chemicals used were of the highest purity available. Water was purified through a Millipore (Bedford, MA) Milli-Q system and used throughout.

Sample Preparation for FRAP Experiments

Concentration of pure EGFP in 20 mM Tris, 0.25 mM EDTA, pH 8.0 buffer was estimated from its molar absorption coefficient (ε) of 53,000 $M^{-1}\ cm^{-1}$ at 489 nm [15] at 25°C. The purity of this solution was confirmed by its absorption and emission spectra that matched those reported previously [15] and by a Western blot analysis using a polyclonal anti-GFP antibody obtained from BD Biosciences Clontech (Palo Alto, CA) that gave a single band on the gel [Kalipatnapu, S., and Chattopadhyay, A., unpublished observations]. Stock solution of EGFP was appropriately diluted in glycerol to achieve a protein concentration of 5 μM in 90% glycerol. This solution was vortexed thoroughly to ensure complete mixing. An aliquot (~5 μL) of this solution was sandwiched between a clean glass slide and a coverslip and sealed with nail enamel and used for imaging and FRAP.

Confocal Microscopy and FRAP Analysis

Fluorescence images of the samples prepared as described earlier were acquired on an inverted Zeiss LSM 510 Meta confocal microscope (Jena, Germany), with a 63×, 1.2 NA water-immersion objective using the 488 nm line of an argon laser at 25°C. Fluorescence emission was collected using the 500–530 nm band pass filter. All images were acquired at a 512 pixel × 512 pixel resolution, and using a 225 μm pinhole. FRAP experiments were carried out by scanning a square region of interest (ROI) and bleaching a circular ROI within this scanned region. Circular bleach ROI of variable radii were obtained using the drawing tool of the software in addition to varying the digital zoom at which images were acquired keeping all other scanning parameters constant. The size of the scan ROI was varied in relation to the dimensions of the bleach

ROI such that for bleach ROI of radii 4.35, 2.9, 2.1, 1.5, 1.4, and 1.0 μm, the scan ROI was a square of length 43.5, 29, 21, 15, 14, and 10 μm, respectively. All images were acquired at a scan speed of 9. Data representing the mean fluorescence intensity recovered in the bleached circular ROI with time were analyzed to determine the characteristic diffusion time (τ_d) based on the model for a uniform-disk illumination condition [21]:

$$F(t) = [F(\infty) - F(0)][\exp(-2\tau_d t^{-1})(I_0(2\tau_d t^{-1}) + I_1(2\tau_d t^{-1}))] + F(0) \quad (1)$$

where $F(t)$ is the normalized mean fluorescence intensity at time t in the bleached ROI, $F(\infty)$ the recovered fluorescence at time $t = \infty$, and $F(0)$ the bleached fluorescence intensity at time $t = 0$. I_0 and I_1 are modified Bessel functions. The bleach time point was calculated as the mid-point of the bleach duration. This resulted in the first post-bleach time point starting from time $t > 0$. The diffusion coefficient (D) is determined from the equation:

$$D = \omega^2(4\tau_d)^{-1} \quad (2)$$

where ω is the actual radius of the bleached ROI. The width of the bleached spot was experimentally determined by fitting the fluorescence intensity profile, obtained using the LSM 510 Meta image analysis software, along a line drawn across the bleached spot to the Gaussian amplitude equation:

$$F = F_0 + Ae^{-(x-x_c)^2/2\omega^2} \quad (3)$$

where F is the pixel fluorescence intensity along a line of distance x drawn across the bleached spot, F_0 the intensity in the unbleached area, x_c the center of bleach, A the amplitude and ω the width. The half-width at half maximum (HWHM) fluorescence intensity was calculated according to the equation:

$$\text{HWHM} = \omega(2 \ln 2)^{0.5} \quad (4)$$

Nonlinear curve fitting of the recovery data to Eq. (1) was carried out using the Graphpad Prism software version 4.00 (San Diego, CA) and to Eq. (3) using the Microcal Origin software version 5.0 (OriginLab Corporation, Northampton, MA)

RESULTS

We monitored the diffusion characteristics of pure EGFP in a 90% glycerol–water mixture using FRAP. Figure 1 represents a sequence of images acquired during a typical FRAP experiment. The glycerol-GFP solution sandwiched between the coverslip and glass slide has a thickness of ~10 μm as estimated by a z-axis scan of the solution in the confocal microscope under the microscope settings described earlier. Photobleaching experiments were carried out by drawing circular ROIs of variable radii and by changing the digital zoom at which the images were acquired. This represents a convenient strategy to carry out photobleaching experiments with a wide range of spot sizes at identical optical resolution, i.e., without using objectives of different numerical apertures. Typical fluorescence recovery plots of EGFP in 90% glycerol bleached with circular ROIs of different radii are shown in Fig. 2. The plots qualitatively indicate that the recovery kinetics is proportional to the radius of the bleach ROI, as is expected from Eq. (2) (i.e., steeper recovery kinetics observed for smaller bleach ROI radii). The kinetics of fluorescence recovery in the bleach ROIs were fit to the model describing FRAP under a uniform-disk illumination condition for photobleaching [21] to arrive at the characteristic diffusion time (τ_d). A linear dependence of τ_d on the square of the bleached spot radius is a stringent criterion to characterize lateral diffusion. As indicated in Fig. 3

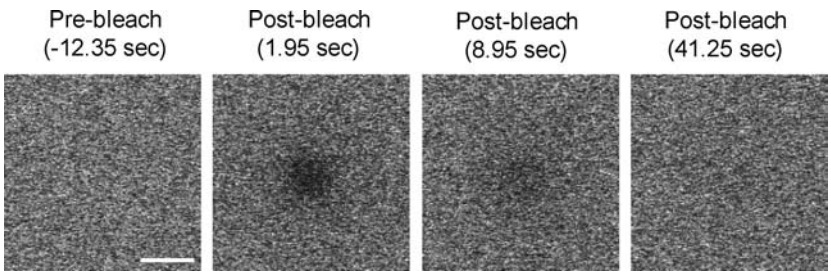

Fig. 1. Panel of images representing a typical FRAP experiment. The panels represent the prebleach and postbleach images of EGFP in 90% glycerol–water mixture acquired at normalized time periods at 25°C. Bleach was carried out in a circular region of interest (ROI) of 4.35 μm radius. Scale bar represents 10 μm. See 'Experimental' section for other details.

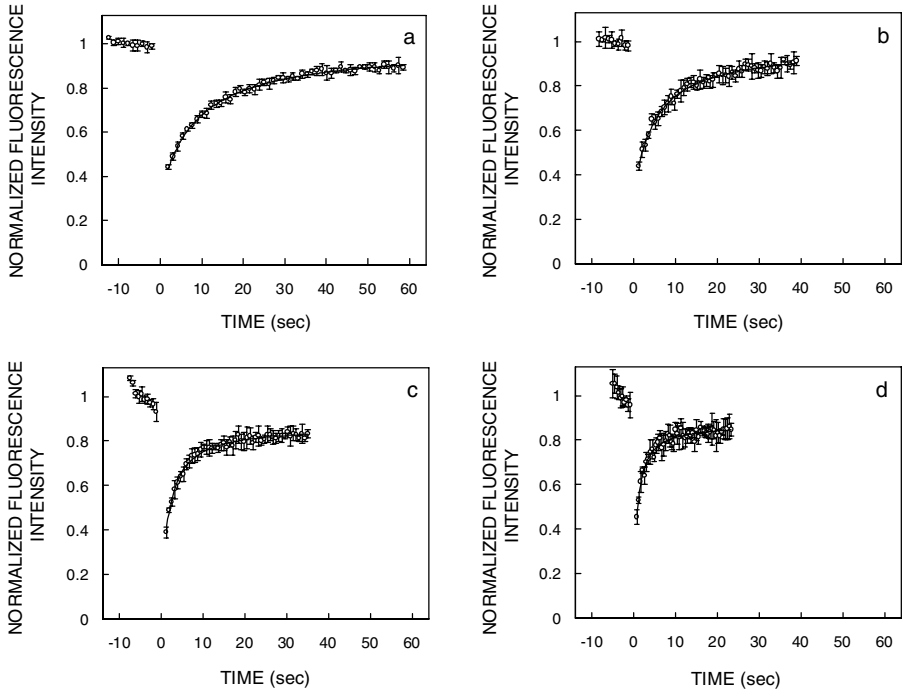

Fig. 2. FRAP recovery plots as a function of bleach spot size. The panels represent the fluorescence recovery kinetics of EGFP in 90% glycerol–water mixture at 25°C when fluorescence was bleached in ROIs of (a) 4.35 μm, (b) 2.9 μm, (c) 1.5 μm, and (d) 1.0 μm radii. The data represent mean ± standard deviation of five independent experiments. The solid lines represent nonlinear regression fits of the data to Eq. (1). The prebleach intensities are shown at time t<0. See 'Experimental' section for other details.

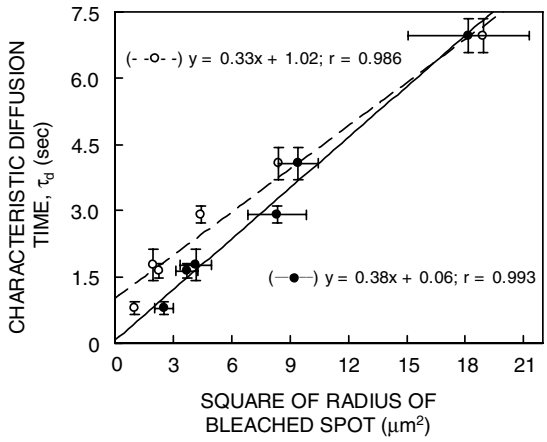

Fig. 3. Dependence of the characteristic diffusion time on the bleach spot size. Characteristic diffusion time (τ_d) of EGFP in 90% glycerol–water mixture at 25°C is plotted as a function of the square of the ROI radius (○) and the square of the calculated half-width at half maximum, HWHM (●). The data represent mean ± standard error of five independent experiments. The lines represent linear regression fits with the fit parameters displayed in the figure.

(open circles), the estimated τ_d of EGFP in 90% glycerol–water mixture indeed shows such dependence when plotted against the square of the actual ROI radii. However, the intercept on the ordinate (y-axis) of the linear fit of this data (dashed line) is a nonzero value (1.02) that does not fulfill the condition of Eq. (2). Moreover, the diffusion coefficient values (D_{ROI}) obtained using the actual ROI radii significantly vary with the ROI radii (see Table I).

The dimensions of the bleached spot is a parameter that significantly affects τ_d and hence the precise determination of diffusion coefficient [22]. In addition, small errors in the estimation of bleach spot sizes are further magnified, since the square of this parameter is utilized in Eq. (2) to arrive at diffusion coefficient values. However, the actual ROI radius represents an instrumental parameter that depends on the pixel resolution, the numerical aperture, and the magnification of the objective that is used to acquire the image. Furthermore, the differences between the refractive index of the sample and the medium (water) used for the immersion objective would be constantly propagated across the entire range of the bleach spot sizes and can not explain the observed variance in τ_D with the ROI radii (Table I). We investigated if a possi-

Table I. FRAP Parameters of EGFP in Glycerol[a]

Actual ROI radius[b] (μm)	Calculated HWHM[c] (μm)	τ_d[d] (s)	D_{ROI}[e] ($\mu m^2\ s^{-1}$)	D_{HWHM}[f] ($\mu m^2\ s^{-1}$)
4.35	4.21±0.39	6.97±0.38	0.68	0.64
2.90	3.06±0.17	4.07±0.36	0.52	0.58
2.10	2.86±0.25	2.91±0.19	0.38	0.70
1.50	1.90±0.15	1.63±0.16	0.35	0.55
1.40	2.00±0.19	1.77±0.36	0.28	0.56
1.00	1.56±0.15	0.79±0.15	0.32	0.77

[a]FRAP experiments were carried out on pure EGFP in 90% glycerol–water mixture under conditions described in 'Experimental' section.
[b]Corresponds to the dimensions of the circular ROI drawn for bleach.
[c]Calculated by nonlinear regression analysis of the fluorescence intensity profiles across the bleached spot to Eq. (3). Data represent the mean ± standard error of five independent experiments. See Figs. 4 and 5 and 'Experimental' section for additional details.
[d]Represents the mean ± standard error of the characteristic diffusion time (τ_d) calculated using Eq. (1) from five independent experiments.
[e]Diffusion coefficient D calculated using the mean τ_d and the actual ROI radii in Eq. (2).
[f]Diffusion coefficient D calculated using the mean τ_d and the mean HWHM in Eq. (2).

ble source for the error in the earlier described linear fits (Fig. 3, dashed lines) and calculated diffusion coefficient based on the ROI radii (D_{ROI}; Table I) are due to an inaccurate determination of the bleach spot size arising due to diffusion of EGFP during bleaching. The first acquired postbleach images of EGFP in 90% glycerol–water mixture for each FRAP experiment performed with different bleach ROI radii were therefore analyzed to determine bleach spot dimensions. Figure 4 represents one such image and shows the fluorescence intensity profile across the bleached spot. Such profiles were fit to the Gaussian amplitude function (Fig. 5) to experimentally determine the HWHM fluorescence intensity of the bleached spots (Table I). The characteristic diffusion time plotted against the square of the experimentally determined HWHM is shown in Fig. 3 (closed circles). The linear fit associated with this data (solid line) yields an intercept on the ordinate (y-axis) that approaches zero (0.06). More importantly, the diffusion coefficient calculated from the slope of this linear fit according to $D = (4\times\text{slope})^{-1}$ yields a value of 0.66 $\mu m^2\ s^{-1}$ that is in agreement with the theoretically predicted diffusion coefficient of 0.7 $\mu m^2\ s^{-1}$ [18].

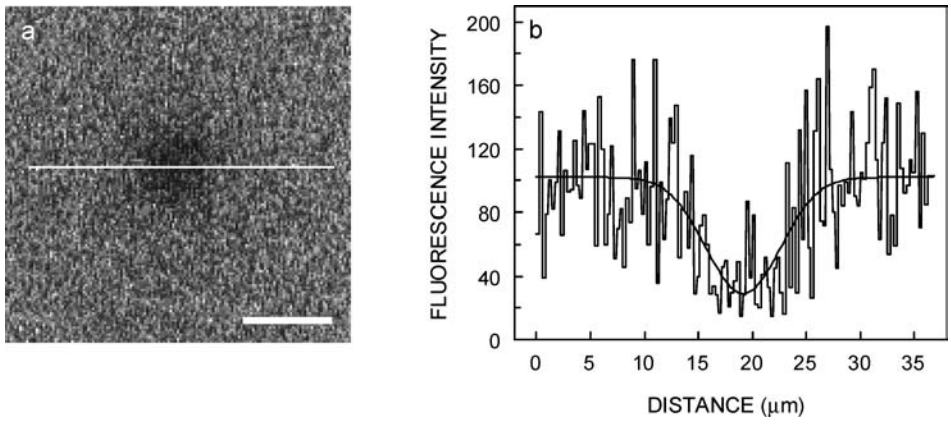

Fig. 4. Typical fluorescence intensity profile across the bleached spot. Panel (a) represents the first acquired postbleach image of EGFP in 90% glycerol–water mixture using an ROI of 4.35 μm radius. The fluorescence intensity profile along the line drawn across the bleached spot is represented in panel (b). The smooth line in panel (b) is a nonlinear regression fit of the data to Eq. (3). Scale bar represents 10 μm. See 'Experimental' section for other details.

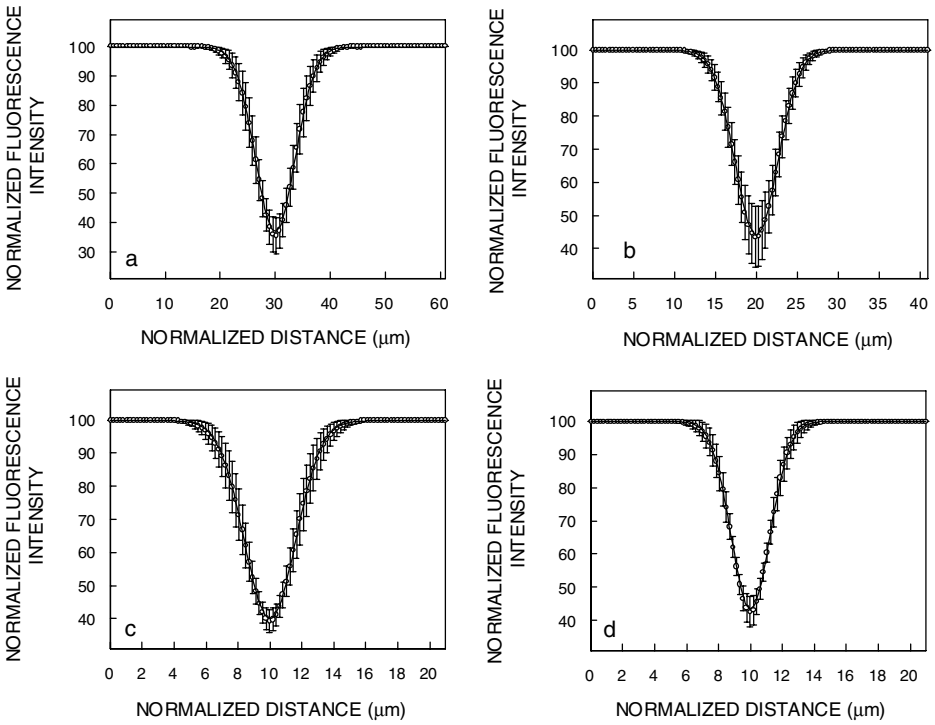

Fig. 5. Gaussian amplitude function fits of the fluorescence intensity profiles across the bleached spot. The panels represent the fluorescence intensity profiles generated from the first acquired postbleach image of EGFP in 90% glycerol–water mixture by bleaching with ROIs of (a) 4.35 μm, (b) 2.9 μm, (c) 1.5 μm, and (d) 1.0 μm radii. The data in each panel represent mean $\pm$ standard deviation of five independently generated nonlinear regression fits of the raw data to Eq. (3). See 'Experimental' section for other details.

The similarity of the experimentally determined diffusion coefficient of EGFP in 90% glycerol–water mixture to that predicted from Stokes–Einstein equation signifies that our data analysis procedure in determining τ_d is accurate, and the experimental determination of the bleached spot dimensions significantly improves the diffusion coefficient estimates in FRAP experiments. It must be mentioned here that the unavoidable instrumental delay in acquiring the first postbleach image would by itself tend to affect the estimation of the bleach spot radius [23,24]. Nevertheless, analysis of the first postbleach image in determining the effective bleach spot dimensions is still justified due to the remarkable improvement in the estimation of diffusion coefficient of EGFP. On a broader perspective, the use of EGFP in 90% glycerol–water mixture as a standard for FRAP experiments appears valid.

The implicit assumption in fluorescence recovery after photobleaching experiments is that the recovery of fluorescence is due to the diffusion of unbleached molecules into the observation region and not due to reversible photobleaching of the fluorophore. Fluorescent proteins like GFP have earlier been reported to exhibit partial reversible photobleaching properties in the millisecond timescale [16]. A recent report indicates that such fluorescent proteins under conditions of low pH display reversible photobleaching properties in the timescale of ~25–60 s [25]. Such phenomena, if existing under the present conditions, would not significantly affect our results for the following reasons. The fast (millisecond timescale) reversible photobleaching process would go undetected due to the relatively long duration between the start of the bleach event and acquisition of the first postbleach image. Furthermore, the longest τ_d we observe for EGFP is ~7 s for the largest ROI (see Table I). Hence, fluorescence recovery due to the slow (~25–60 s) reversible photobleaching process would be negligible with the predominant contribution to the recovery in fluorescence coming from diffusion of EGFP molecules into the observation region. Importantly, since reversible photobleaching is an intrinsic property of the fluorophore, its recovery kinetics would be independent of the area bleached in FRAP experiments. Hence, the linear dependence of τ_d of EGFP to the size of the bleached area (Fig. 3) would exclude the possibility of a significant contribution in the fluorescence recovery due to reversible

photobleaching of EGFP. In addition, the present experiments with EGFP have been performed at high pH (8.0) conditions that would significantly reduce the probability for reversible photobleaching of EGFP.

DISCUSSION

We have monitored diffusion characteristics of EGFP in a glycerol–water mixture using the technique of FRAP with an overall objective of validating GFP-based fluorophores as suitable markers for FRAP measurements. The molecular characteristics of GFP such as its relative photostability, well-defined photobleaching behavior, relative insensitivity of the lateral diffusion coefficient over a broad range of protein concentrations and the relative invariance of the bleach extents to solutes such as oxygen [16] render it suitable for FRAP applications. Importantly, the theoretically predicted diffusion coefficient of GFP in a solution of viscosity comparable to that of a 90% glycerol–water mixture falls in a range that is easily measurable using standard confocal microscopes and is experimentally verified in the present work. In addition, the widespread use of purified GFP as a standard in electrophoresis and fluorescence assisted cell sorting (FACS) applications makes it an easily available fluorescent marker in most laboratories.

Our results indicate that τ_d values obtained for EGFP in 90% glycerol–water mixture vary linearly with the square of the bleached area, a necessary condition that characterizes lateral diffusion. Interestingly, the fit parameters of this plot match the ones predicted from theory more closely when the experimentally determined bleached spot radii (HWHM) are used instead of the actual ROI radii. In principle, the bleach duration in a FRAP experiment must be instantaneous or infinitely small compared to τ_d of the fluorophore in a given system [26]. On account of the finite time period required to repeatedly scan and hence induce a significant extent of bleach in an ROI, a condition that is true for most confocal FRAP experiments [24], our experiments unavoidably resulted in bleach durations that were ~40–160% of τ_d. A bleach duration longer than τ_d of the fluorophore in a particular system can induce formation of a 'corona' around the bleached region. This occurs due to repeated photobleaching of fluorophores adjacent to the bleach region on account of their diffusion into the bleach region [23, 24], thus resulting in fluorescence loss on repeated photobleaching. This effectively increases the bleached spot size, resulting in an underestimation of the diffusion coefficient. Our results indicate that this effect, while unavoidable in the present experiments, can be corrected by experimentally determining the bleach spot dimensions through image analysis of the first acquired postbleach image. Thus, the plot of the square of the 'corrected' bleach spot dimensions (HWHM) against τ_d gives a better linear fit and a diffusion coefficient of 0.66 $\mu m^2\ s^{-1}$, which is in agreement with the theoretical value of 0.7 $\mu m^2\ s^{-1}$. For a molecule undergoing diffusion at a constant rate, bleaching a smaller ROI would result in faster recovery kinetics which would cause a larger increase in the effective bleached spot. This is evident from Fig. 3 wherein the deviation between the plots of the actual ROIs vs. τ_d (dashed line) and the corrected bleach spot (HWHM) vs. τ_d (solid line) is more pronounced for smaller bleach ROIs.

It must be mentioned here that the lateral diffusion of GFP in aqueous and/or water–glycerol mixtures measured earlier using FRAP has yielded values similar to those predicted from theory [16,18]. Our present work represents a more comprehensive analysis (using a wide range of bleach spot sizes) of this system. Moreover, it has been possible to accurately determine the diffusion coefficients of GFP in solutions of varying viscosities in some of these cases (for e.g., see Ref. [16]) primarily with the use of a specialized microscope set-up that can induce bleaching of GFP in a remarkably short duration of time. Such an experimental set-up, although highly desirable, is not available and practical in most laboratories. In this regard, our FRAP experiments performed on a commercially available and widely used confocal microscope with standard data acquisition configuration assumes significance. Importantly, our results indicate that even under conditions of reduced mobility of GFP (such as in a water–glycerol mixture), routine FRAP experiments with small bleach spot dimensions invariably tend to underestimate its diffusion coefficient. These estimates can be corrected to a significant extent by analyzing the effective bleached spot size obtained in such FRAP experiments by relatively simple image analysis procedures. We therefore believe that the results presented in our manuscript are appropriate for the accurate analysis of diffusion parameters of molecules and would contribute to the popularity of the technique of FRAP performed on commercially available confocal microscopes. Our results therefore are relevant to the growing literature on corrective measures necessary for the accurate determination of diffusion coefficients using confocal FRAP measurements [23,24]. Moreover, the analysis of GFP diffusion in a viscous medium with a range of bleach spot sizes has provided us with an appropriate experimental framework in which to analyze the diffusion properties of more complex systems such as the mobility of the G-protein coupled serotonin$_{1A}$ receptor in the plasma membrane of living cells [12]. Taken together, these results demonstrate the applicability of GFP in viscous solutions as a standard for FRAP experiments.

ACKNOWLEDGMENTS

This work was supported by the Council of Scientific and Industrial Research, Government of India. T.J.P. thanks the Council of Scientific and Industrial Research for the award of a Senior Research Fellowship. A.C. is an Honorary Faculty Member of the Jawaharlal Nehru Centre for Advanced Scientific Research, Bangalore (India). We sincerely thank Prof. G. Krishnamoorthy (Tata Institute for Fundamental Research, Mumbai, India) for the kind gift of purified EGFP. We thank Nandini Rangaraj, V.K. Sarma, N.R. Chakravarthi and K.N. Rao for technical help during confocal microscopy. We thank members of our laboratory for critically reading the manuscript.

REFERENCES

1. N. O. Petersen, S. Felder, and E. L. Elson (1986). In D. M. Weir, L. A. Herzenberg, C. C. Blackwell, and L. A. Herzenberg (Eds.) *Measurement of Lateral Diffusion by Fluorescence Photobleaching Recovery*, Blackwell Scientific Publications, Edinburgh, pp. 24.1–24.23.
2. D. E. Wolf (1989). In D. L. Taylor, and Y.-L. Wang (Eds.) *Designing, Building, and Using a Fluorescence Recovery After Photobleaching Instrument*, Academic Press, New York, pp. 271–306.
3. M. Edidin (1994). In S. Damjanovich, M. Edidin, J. Szollosi, and L. Tron (Eds.) *Fluorescence Photobleaching and Recovery, FPR, in the Analysis of Membrane Structure and Dynamics*, CRC Press, Boca Raton, Florida, pp. 109–135.
4. G. M. Lee and K. Jacobson (1994). In A. Kleinzeller and D. M. Fambrough (Eds.) *Lateral Mobility of Lipids in Membranes*, Academic Press, New York, pp. 111–142.
5. J. Lippincott-Schwartz, E. Snapp, and A. Kenworthy (2001). Studying protein dynamics in living cells. *Nat. Rev. Mol. Cell Biol.* **2**, 444–456.
6. M. Weiss and T. Nilsson (2004). In a mirror dimly: Tracing the movements of molecules in living cells. *Trends Cell Biol.* **14**, 267–273.
7. R. Y. Tsien (1998). The green fluorescent protein. *Annu. Rev. Biochem.* **67**, 509–544.
8. J. C. G. Blonk, A. Don, H. Van Aalst, and J. J. Birmingham (1993). Fluorescence photobleaching recovery in the confocal scanning light microscope. *J. Microsc.* **169**, 363–374.
9. D. Axelrod, D. E. Koppel, J. Schlessinger, E. Elson, W. W. Webb (1976). Mobility measurement by analysis of fluorescence photobleaching recovery kinetics. *Biophys. J.* **16**, 1055–1069.
10. N. L. Thompson and D. Axelrod (1980). Reduced lateral mobility of a fluorescent lipid probe in cholesterol-depleted erythrocyte membrane. *Biochim. Biophys. Acta* **597**, 155–165.
11. L. Kallal and J. L. Benovic (2000). Using green fluorescent proteins to study G-protein-coupled receptor localization and trafficking. *Trends Pharmacol. Sci.* **21**, 175–180.
12. T. J. Pucadyil, S. Kalipatnapu, K. G. Harikumar, N. Rangaraj, S. S. Karnik, and A. Chattopadhyay (2004). G-protein-dependent cell surface dynamics of the human serotonin$_{1A}$ receptor tagged to yellow fluorescent protein. *Biochemistry* **43**, 15852–15862.
13. T. J. Pucadyil, S. Kalipatnapu, and A. Chattopadhyay (2005). Membrane organization and dynamics of the G-protein coupled serotonin$_{1A}$ receptor monitored using fluorescence-based approaches, *J. Fluoresc. 15*, 785–796.
14. R. Heim and R. Y. Tsien (1996). Engineering green fluorescent proteins for improved brightness, longer wavelengths and fluorescence resonance energy transfer. *Curr. Biol.* **6**, 178–182.
15. G. H. Patterson, S. M. Knobel, W. D. Sharif, S. R. Kain, and D. W. Piston (1997). Use of green fluorescent protein and its mutants in quantitative fluorescence microscopy. *Biophys. J.* **73**, 2782–2790.
16. R. Swaminathan, C. P. Hoang, and A. S. Verkman (1997). Photobleaching recovery and anisotropy decay of green fluorescent protein GFP-S65T in solution and cells: cytoplasmic viscosity probed by green fluorescent protein translational and rotational diffusion, *Biophys. J.* **72**, 1900–1907
17. M. Ormö, A. B. Cubitt, K. Kallio, L. A. Gross, R. Y. Tsien, and S. J. Remington (1996). Crystal structure of the *Aequorea victoria* green fluorescent protein. *Science* **273**, 1392–1395.
18. U. Kubitscheck, O. Kückman, T. Kues, and R. Peters (2000). Imaging and tracking of single GFP molecules in solution. *Biophys. J.* **78**, 2170–2179.
19. P. F. F. Almeida and W. L. C. Vaz (1995). In R. Lipowsky and E. Sackmann (Eds.) *Lateral Diffusion in Membranes*, Elsevier Science, Amsterdam, pp. 305–357.
20. T.-T. Yang, L. Cheng, and S. R. Kain (1996). Optimized codon usage and chromophore mutations provide enhanced sensitivity with the green fluorescent protein. *Nucleic Acids Res.* **24**, 4592–4593.
21. D. M. Soumpasis (1983). Theoretical analysis of fluorescence photobleaching recovery experiments. *Biophys. J.* **41**, 95–97.
22. N. Klonis, M. Rug, I. Harper, M. Wickham, A. Cowman, and L. Tilley (2002). Fluorescence photobleaching analysis for the study of cellular dynamics. *Eur. Biophys. J.* **31**, 36–51.
23. M. Weiss (2004). Challenges and artifacts in quantitative photobleaching experiments, *Traffic* **5**, 662–671.
24. J. Braga, J. M. P. Desterro, and M. Carmo-Fonseca (2004). Intracellular macromolecular mobility measured by fluorescence recovery after photobleaching with confocal laser microscopes. *Mol. Biol. Cell* **15**, 4749–4760.
25. D. Sinnecker, P. Voigt, N. Hellwig, and M. Schaefer (2005). Reversible photobleaching of enhanced green fluorescent proteins. *Biochemistry* **44**, 7085–7094.
26. A. Lopez, L. Dupou, A. Altibelli, J. Trotard, and J. F. Tocanne (1988). Fluorescence recovery after photobleaching (FRAP) experiments under conditions of uniform disk illumination. Critical comparison of analytical solutions, and a new mathematical method for calculation of diffusion coefficient D. *Biophys. J.* **53**, 963–970.